Article:

Rizzelli, S.L., Jones, E.R., Thompson, K.L. et al. (2015) Preparation of non-aqueous Pickering emulsions using anisotropic block copolymer nanoparticles. Colloid and Polymer Science , 294 (1). pp. 1-12. ISSN: 0303-402X

https://doi.org/10.1007/s00396-015-3785-3

Preparation of Non-Aqueous Pickering Emulsions Using Anisotropic Block Copolymer Nanoparticles

Journal:	*Colloid and Polymer Science*
Manuscript ID	CPS-2015-0441.R2
Manuscript Type:	Original Contribution
Date Submitted by the Author:	14-Sep-2015
Complete List of Authors:	Rizzelli, Silvia; The University of Sheffield, Chemistry Jones, Elizabeth; The University of Sheffield, Chemistry Thompson, Kate; The University of Sheffield, Chemistry Armes, Steve; Sheffield University, Chemistry
Keywords:	RAFT polymerization, self-assembly, Pickering emulsions, non-aqueous emulsions, block copolymers, nanoparticles, dispersion polymerization

Preparation of Non-Aqueous Pickering Emulsions Using Anisotropic Block Copolymer Nanoparticles

S. L. Rizzelli, E. R. Jones, K. L. Thompson and S. P. Armes*

Abstract.

In this work we show that amphiphilic diblock copolymer worms prepared via alcoholic RAFT dispersion polymerization can be used to stabilize non-aqueous Pickering emulsions. A previously reported synthesis protocol based on polymerization-induced self-assembly (PISA) was modified to enable the preparation of poly(2-(dimethylamino) ethyl methacrylate)-poly(benzyl methacrylate) (PDMA-PBzMA) worm-like particles directly in methanol at relatively high solids. A dilute dispersion of these highly anisotropic nanoparticles was then homogenized with sunflower oil to produce sunflower oil-in-methanol emulsions. The mean droplet diameter ranged from 9 to 104 μm, depending on the nanoparticle concentration and the stirring rate used for homogenization. The sunflower oil content was increased systematically, with stable emulsions being obtained up to a volume fraction of 0.60. In all cases, the sunflower oil droplets gradually increase in size on ageing for up to four days. However, stable emulsions were obtained after this time period, with no further change in the mean droplet diameter for at least two months on standing at ambient temperature. Turbidimetry studies of the continuous phase after sedimentation of the relatively dense emulsion droplets indicated that the initial adsorption efficiency of the PDMA-PBzMA worms is very high, but this is reduced significantly as the droplet diameter gradually increases during ageing. There is a concomitant increase in fractional surface coverage over the same time period, suggesting that the increase in droplet diameter is the result of limited coalescence, rather than an Ostwald ripening mechanism.

Keywords. RAFT polymerization, self-assembly, Pickering emulsions, non-aqueous emulsions, block copolymers, nanoparticles.

Steven P. Armes
Department of Chemistry, Dainton Building, University of Sheffield, Brook Hill, Sheffield, Yorkshire, S3 7HF, UK.
e-mail: s.p.armes@sheffield.ac.uk

Introduction

A Pickering emulsion comprises either oil or water droplets that are stabilized by solid particles adsorbed at the oil/water interface. This type of emulsion was first reported by Ramsden over a century ago [1] but Pickering's subsequent studies received more credit and led to today's nomenclature [2]. Various classes of solid particles have been employed as Pickering emulsifiers, including silica [3-7], inorganic clays [8-12] and organic polymer latexes [13-18]. Either oil-in-water (o/w) or water-in-oil (w/o) Pickering emulsions can be obtained, with the emulsion type mainly depending on the contact angle (θ) between the particles and the interface. Thus hydrophilic particles possess contact angles less than 90 ^{o} and reside in the aqueous phase, favoring the stabilization of o/w emulsions. In contrast, hydrophobic particles are characterized by contact angles greater than 90 ^{o} and hence are preferentially located within the oil phase, resulting in the formation of w/o emulsions.

The main driving force for the interfacial adsorption of particles is the reduction in surface area. The energy required to detach spherical particles adsorbed at the interface is dictated by the contact angle and the particle radius [19,20]. In many cases, larger particles can be considered to be essentially irreversibly adsorbed, since the detachment energy is several orders of magnitude greater than the particle thermal energy [19,20]. Since the adsorbed particle layer prevents droplet coalescence by providing a strong steric barrier, Pickering emulsions tend to be far more stable than surfactant-stabilized emulsions [21]. Moreover, Pickering emulsions also offer several other advantages, such as reduced foaming during homogenization, more reproducible formulations and lower toxicity [20,21].

Although far less commonly reported than w/o or o/w emulsions, there are various examples of non-aqueous emulsions in the literature [22-26]. Such systems require a pair of immiscible solvents [27]. In principle, non-aqueous emulsions could be utilized for water-sensitive reactions or polymerizations [26,28,29], for reactions that need to be conducted above the normal boiling point of water [30] or for specific applications where the presence of water is problematic [31,32].

In 2004 two research groups led by Paunov and Velev reported the formation of colloidosomes, Pickering emulsions and foams stabilized using 'polymeric microrods' [33,34], rather than conventional spherical particles. These microrods were prepared from epoxy-type photoresist SU-8 using the liquid-lquid dispersion technique and possessed relatively large dimensions (mean rod length = 23.5 μm; mean rod width = 0.6 μm). More recently, we have described the use of much smaller hydrophilic diblock copolymer worms as Pickering emulsifiers for the preparation of o/w [35] or w/o [36] emulsions. In principle, such highly anisotropic particles should be more strongly adsorbed than precursor spherical particles (i.e. whose mean diameter is comparable to the mean worm width). Other research teams have also reported that anisotropic particles are highly effective Pickering emulsifiers [37,38]. For example, Madivala et al. found that the emulsion droplet stability depended strongly on the particle aspect ratio when using elongated hematite or polystyrene latex particles [39]. Similarly, a recent study by Kalashnikova et al. reported the use of cellulose nanorods to form Pickering emulsions. Interestingly, it was found that too high an aspect ratio enabled these particles to adsorb simultaneously onto multiple droplets, rather than stabilizing individual droplets [40].

The recent development of living radical polymerization techniques [41-46] has provided a facile route for the production of diblock copolymer nanoparticles based on polymerization-induced self-assembly (PISA) [47-54]. In particular, the ability to form well-defined amphiphilic diblock copolymers via reversible addition-fragmentation chain transfer (RAFT) polymerization under appropriate reaction conditions allows the *in situ* formation of copolymer nanoparticles with either spherical, worm-like or vesicular morphologies [52,55-59]. Moreover, this approach has proven to be highly versatile, with all three copolymer morphologies being reported as pure phases in either water [52,60,61], alcohol [55,58,62-65] or *n*-alkanes [59,66,67]. Aqueous emulsion polymerization has been extensively researched by Charleux and co-workers [50,68-74]. However, RAFT dispersion polymerization formulations are arguably rather more generic [58,59,61,62,64,65,75-80]. Of particular relevance to the present study, Thompson et al. have recently shown that block copolymer worms prepared via RAFT PISA are effective stabilizers for non-aqueous emulsions comprising ethylene glycol droplets within various *n*-alkanes [81]. Herein we utilize a RAFT PISA formulation to conveniently prepare diblock copolymer worms directly in methanol. These flexible, highly anisotropic nanoparticles are then examined as putative Pickering emulsifiers for the preparation of new non-aqueous emulsions composed of sunflower oil droplets dispersed in a methanolic continuous phase. Thus this new non-aqueous emulsion formulation is complementary to that reported by Thompson et al. [81].

Materials and methods

Ethanol was obtained from VWR Chemicals (UK) and *n*-hexane was purchased from Fisher Scientific (UK). All other reagents were purchased from Sigma-Aldrich (UK) and were used as received unless otherwise noted. Either 4,4'-Azobis(4-cyanovaleric acid) (ACVA) or 2,2'-azobis(isobutyronitrile) (AIBN) were used as initiators. Benzyl methacrylate (BzMA) (96%; Sigma Aldrich) was passed through an inhibitor removal column prior to use. 4-Cyano-4-(2-phenylethanesulfanylthiocarbonyl) sulfanylpentanoic acid (PETTC) was prepared in-house as reported previously [79].

Synthesis of poly(2-(dimethylamino)ethyl methacrylate) (PDMA) macro-CTA agent. A round-bottomed flask was charged with 2-(dimethylamino)ethyl methacrylate (DMA; 40.0 g, 254 mmol), PETTC (2.156 g, 6.36 mmol; target DP = 40), ACVA (178 mg, 0.636 mmol; PETTC/ACVA molar ratio = 10) and THF (40.0 g). The sealed reaction vessel was purged with nitrogen and placed in a pre-heated oil bath at 66 ˚C for 6 h. The resulting crude PDMA (monomer conversion = 77%; M_n = 6,500 g mol^{-1}, M_w/M_n = 1.22) was purified by precipitation into excess petroleum ether. The mean degree of polymerization (DP) of this PDMA macro-CTA was calculated to be 43 using ^{1}H NMR spectroscopy by comparing the integrated signals corresponding to the aromatic protons at 7.2 - 7.4 ppm with those assigned to the methacrylic polymer backbone at 0.4 - 2.5 ppm.

Synthesis of poly(2-(dimethylamino)ethyl methacrylate)-poly(benzyl methacrylate) (PDMA-PBzMA) diblock copolymer particles via dispersion polymerization in methanol. In a typical RAFT dispersion polymerization synthesis conducted at 15 % w/w total solids, BzMA (2.0 g, 11.4 mmol), PDMA$_{43}$ macro-CTA (0.85 g, 0.119 mmol; target DP = 95) and AIBN (3.9 mg, 0.024 mmol; macro-CTA/AIBN molar ratio = 5) were dissolved in methanol (16.16 g). The reaction mixture was sealed in a round-bottomed flask, purged with nitrogen gas for 15 min, and then placed in a preheated oil bath at 64 ºC for 24 h. The final monomer conversion was determined by ^{1}H NMR analysis by comparing the integral due to the two benzylic protons assigned to the PBzMA block at 4.9 ppm to that of the BzMA monomer vinyl signals at 5.2 and 5.4 ppm.

Copolymer characterization. Diblock copolymer molecular weight distributions were assessed using gel permeation chromatography (GPC). The GPC set-up comprised two 5 µm (30 cm) 'Mixed C' columns and a WellChrom K-2301 refractive index detector operating at 950 ± 30 nm. THF eluent contained 2.0 % v/v triethylamine and 0.05 % w/v butylhydroxytoluene (BHT) was used at a flow rate of 1.0 ml min^{-1}. A series of ten near-monodisperse linear poly(methyl methacrylate) standards (M_p ranging from 1,280 to 330,000 g mol^{-1}) were purchased from Polymer Laboratories (Church Stretton, UK) and employed for calibration using the above refractive index detector.

^{1}H NMR spectra were acquired on a Bruker 400 MHz spectrometer in either $CDCl_3$ or CD_2Cl_2. All chemical shifts are reported in ppm (δ). DLS measurements were conducted using a Malvern Instruments Zetasizer Nano series instrument equipped with a 4 mW He-Ne laser operating at 633 nm, an avalanche photodiode with high quantum efficiency, and an ALV/LSE-5003 multiple tau digital correlator electronics system.

TEM studies were conducted using a Philips CM 100 instrument operating at 100 kV equipped with a Gatan 1k CCD camera. Solutions were diluted with methanol at 20 ºC to generate 0.20 % w/w dispersions. Copper/palladium TEM grids (Agar Scientific, UK) were surface-coated in-house to yield a thin film of amorphous carbon. The grids were then plasma glow-discharged for 30 seconds to create a hydrophilic surface. Each methanolic diblock copolymer dispersion (0.20 % w/w, 10 µL) was placed onto a freshly glow-discharged grid for 1 min and then blotted with filter paper to remove excess solution. To stain the deposited nanoparticles, 10 µL of a 0.75 % w/w aqueous solution of uranyl formate was placed on the sample-loaded grid via micropipet for 20 seconds and then carefully blotted to remove excess stain. Each grid was then carefully dried using a vacuum hose.

Preparation of Pickering emulsions. Sunflower oil (5.0 ml) was homogenized with 5.0 ml of a 0.01-2.65 % w/w methanol copolymer dispersion for 2 min at 20 ºC using a IKA Ultra-Turrax T-18 homogenizer equipped with a 10 mm dispersing tool

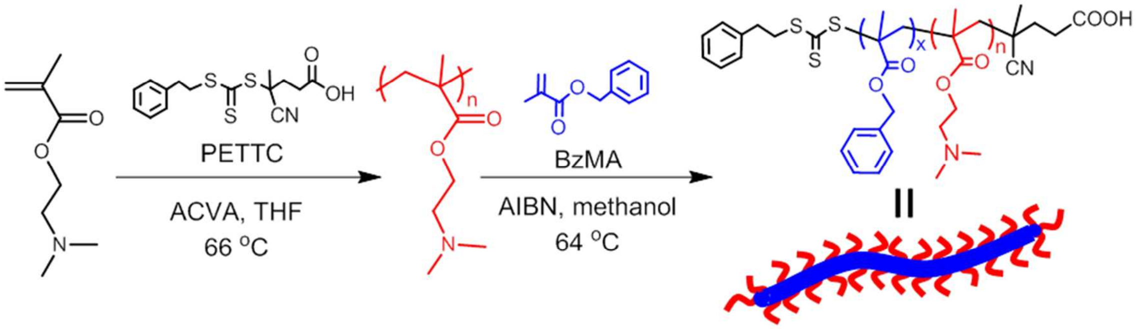

Scheme 1 Chain extension of a poly(2-(dimethylamino)ethyl methacrylate) (PDMA) macro-CTA with benzyl methacrylate (BzMA) via RAFT alcoholic dispersion polymerization at 64 ºC to produce sterically-stabilized PDMA-PBzMA diblock copolymer worm-like nanoparticles via polymerization-induced self-assembly (PISA)

operating at between 3,500 and 13,500 rpm. Between samples the homogenizer was washed thoroughly using methanol to ensure that there was no contamination of the samples.

Optical microscopy. Optical microscopy images of Pickering emulsion droplets were recorded using a Motic DMBA300 digital biological microscope equipped with a built-in camera and analyzed using Motic Images Plus 2.0 ML software.

Laser diffraction. Each emulsion was sized in methanol using a Malvern Mastersizer 2000 instrument equipped with a small volume Hydro 2000SM sample dispersion unit (ca. 50 ml), a He-Ne laser operating at 633 nm and a solid-state blue laser operating at 466 nm. The stirring rate was adjusted to 500 rpm in order to avoid droplet coalescence. After each measurement, the cell was rinsed once with doubly-distilled water, followed by rinsing with first ethanol and then methanol. The glass walls of the cell were carefully wiped with lens cleaning tissue to avoid cross-contamination and the laser was aligned centrally to the detector prior to data acquisition.

Determination of Pickering emulsifier adsorption efficiency via turbidimetry. UV spectra were recorded at 20 ˚C for the $PDMA_{43}$-$PBzMA_{94}$ worms in methanol using a Shimadzu UV-1800 instrument operating between 400 and 800 nm. A linear calibration plot of absorbance versus concentration at an arbitrary wavelength of 430 nm with known concentrations of copolymer dispersed in methanol was constructed in order to determine the nanoparticle adsorption efficiency at the oil-ethanol interface. This was assessed by analysis of the (upper) methanol continuous phase after sedimentation of the relatively dense sunflower oil droplets had occurred on standing for 24 h (or longer) at 20 ˚C. The remaining non-adsorbed worms were detected and thus the fraction of adsorbed worms was calculated by difference.

Results and Discussion

PDMA-PBzMA diblock copolymer nanoparticles were synthesized by RAFT alcoholic dispersion polymerization of benzyl methacrylate (BzMA) in methanol at 64 ˚C, see Scheme 1. A similar ethanolic PISA formulation has been recently reported [58,64]. Unfortunately, ethanol is miscible with most oils of interest, hence methanol was selected as the continuous phase since this more polar solvent was more likely to allow the preparation of non-aqueous emulsions. As for the earlier ethanolic PISA formulation reported by our group, if the PDMA stabilizer block was sufficiently short, a range of nanoparticle morphologies could be produced by simply varying the mean degree of polymerization of the core-forming PBzMA block, see Figure 1.

For this study, worm-like micelles was the desired copolymer morphology. Such highly anisotropic nanoparticles can be obtained by targeting a mean PBzMA DP of 95. Approximately 99% BzMA conversion was achieved within 24 h as judged by ^{1}H NMR spectroscopy, which suggested a mean DP of 94 for the core-forming PBzMA block. THF GPC indicated a mean number-average molecular weight of 12800 g mol^{-1} and a polydispersity (M_w/M_n) of 1.08. The representative TEM images shown in Figure 1B and 1D confirm a well-defined worm morphology, with a mean worm width of 20 nm.

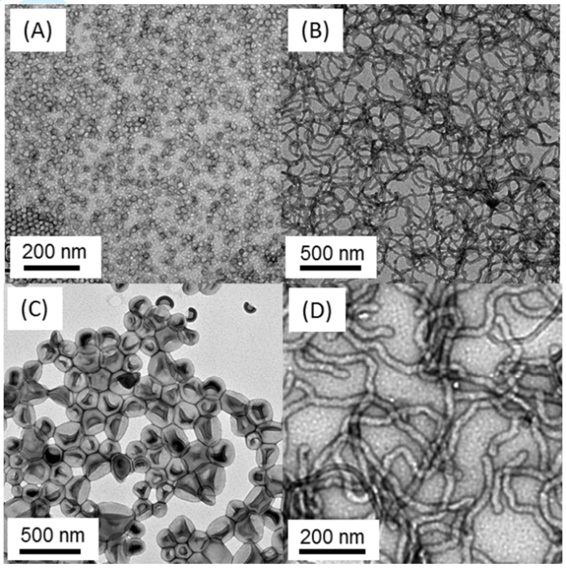

Fig. 1 TEM images obtained for $PDMA_{43}$-$PBzMA_x$ diblock copolymer nanoparticles prepared at 15 % w/w solids via RAFT dispersion polymerization of BzMA in methanol at 64 ºC using a $PDMA_{43}$ macro-CTA, AIBN initiator, and a [macro-CTA]/[AIBN] molar ratio of 5.0. Varying the DP of the core-forming PBzMA results in either (A) spheres (x = 60), (B) worms (x = 94) or (C) vesicles (x = 200). (D) Higher magnification image of (B), indicating a mean worm width of 20 nm

Table 1 Attempted Pickering emulsification of various oils using a methanolic dispersion containing 0.66 % w/w PDMA$_{43}$-PBzMA$_{94}$ diblock copolymer worms. Homogenization conditions: 13500 rpm for 2 minutes at 20 ˚C with a sunflower oil volume fraction of 0.50

Oil phase	Emulsion	Comments
Sunflower Oil	Yes	Stable emulsion
***n*-Octane**	No	Initial emulsion, but demulsified after 2-3 h
***n*-Dodecane**	No	Complete phase separation
***n*-Tetradecane**	No	Complete phase separation
***n*-Hexadecane**	No	Complete phase separation
Isopropyl myristate	No	Miscible with methanol

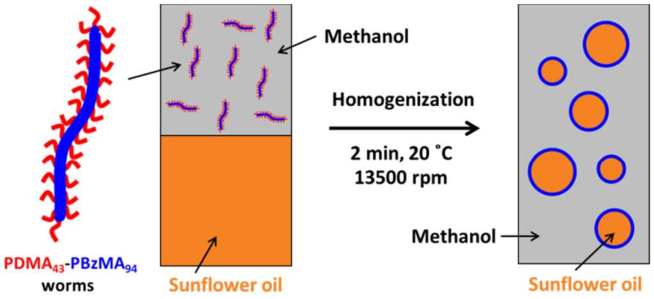

Scheme 2 Homogenization of 0.66 % w/w PDMA$_{43}$-PBzMA$_{94}$ diblock copolymer worms in methanol with sunflower oil at 13500 rpm at 20 ºC for 2 min produces stable sunflower oil-in-methanol Pickering emulsions

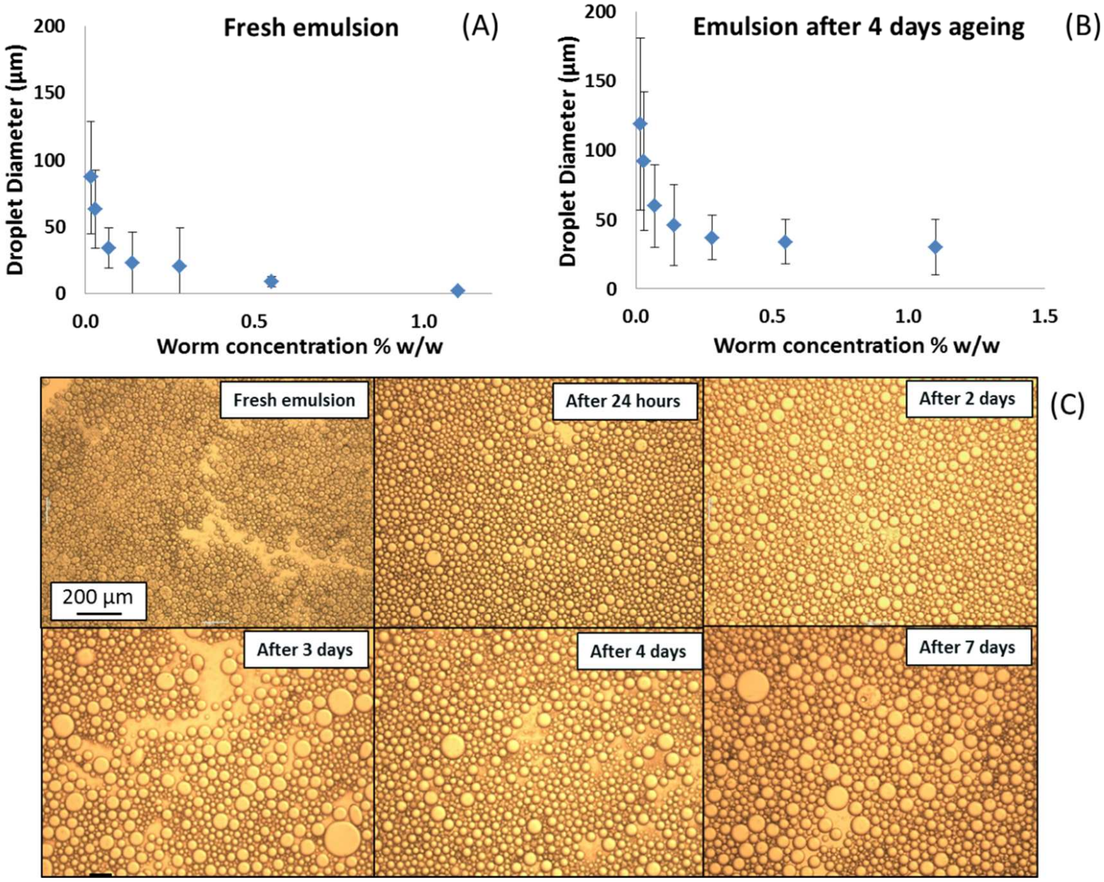

Fig. 2 (A) Mean droplet diameter versus copolymer concentration for the PDMA$_{43}$-PBzMA$_{94}$ worms for the freshly prepared emulsion and (B) the same emulsions after four days standing at 20 °C, as determined using laser diffraction. In both cases the error bars represent the standard deviation of each mean volume-average droplet diameter, rather than the experimental error. (C) Optical microscopy images recorded for the fresh and aged emulsions at 0.66 % w/w worm concentration measured over a period of seven days. The 200 µm scale bar in the first image applies to all images

However, the worms exhibit considerable polydispersity in length, ranging from less than 1 µm up to around 5 µm, as estimated from TEM images. This is typical for such PISA syntheses, since the worms are formed via random sphere-sphere fusion events during the *in situ* RAFT polymerization. A sphere-equivalent hydrodynamic diameter of 609 nm (polydispersity = 0.50) was determined at 25 ˚C using dynamic light scattering (DLS). [N.B. DLS measurements are based on the Stokes-Einstein equation, which assumes a spherical particle morphology; hence the data obtained for such highly anisotropic worms should be treated with caution.] THF GPC data recorded for the final diblock copolymer indicates a relatively high blocking efficiency for the PDMA macro-CTA and a narrow molecular weight distribution, which are consistent with a well-controlled RAFT polymerization. Various oils were evaluated for homogenization with the methanolic copolymer dispersion, see Table 1. A range of *n*-alkanes were evaluated in addition to sunflower oil. However, for *n*-octane, *n*-dodecane, *n*-tetradecane or *n*-hexadecane, emulsions were only stable for a few hours, if formed at all. In contrast, Pickering emulsions with good long-term stability could be consistently obtained using sunflower oil.

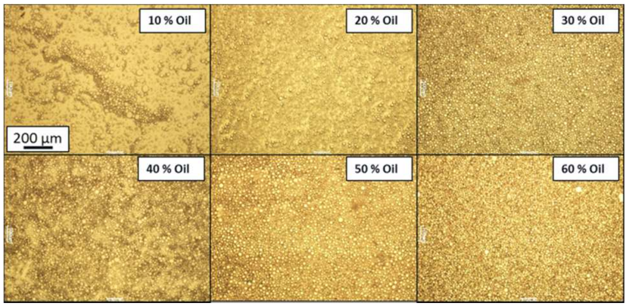

Fig. 3 Optical microscopy images recorded for sunflower oil-in-methanol Pickering emulsions prepared using 0.66 % w/w $PDMA_{43}$-$PBzMA_{94}$ worms at sunflower oil volume fractions of between 0.10 and 0.60. The 200 µm scale bar shown in the first image applies to all images

Thus only this latter oil was selected for further studies. Scheme 2 depicts the schematic representation of the formation of a $PDMA_{43}$-$PBzMA_{94}$ worm-stabilized sunflower oil-in-methanol Pickering emulsion. Figure 2A shows how the sunflower oil diameter varies with $PDMA_{43}$-$PBzMA_{94}$ worm concentration; these laser diffraction measurements were recorded immediately after homogenization. Figure 2B shows the same trend, but in this case measurements were recorded on four-day-old emulsions. Optical microscopy images (see Figure S1) support the data sets shown in Figures 2A and 2B: lower particle concentrations produce larger sunflower oil droplets. This relationship has been reported for many other Pickering emulsions [35]. This is because there are more nanoparticles available to coat and stabilize the oil droplet surface at higher copolymer concentrations, thus enabling the formation of smaller droplets. At a copolymer concentration of 0.66 % w/w, the freshly-made emulsions had a volume-average droplet diameter of 9 ± 6 µm, as judged by laser diffraction. However, this mean diameter increased up to 39 ± 21 µm on standing at 20 ˚C for four days. Following this discovery, fresh emulsions were prepared and the evolution in the droplet diameter was monitored daily. After four days, no further increase in droplet diameter was observed and the resulting relatively coarse emulsions remained stable for at least two months on storage at 20 ˚C, optical microscopy images recorded over a period of seven days are shown in Figure 2C.

The sunflower oil volume fraction was systematically varied between 0.10 and 0.90 to assess the efficiency of emulsification. Stable emulsions were formed up to an oil volume fraction of 0.60; using higher volume fractions of sunflower oil did not produce stable emulsions. Figure 3 shows the optical microscopy images obtained for a series of emulsions prepared using 0.66 % w/w $PDMA_{43}$-$PBzMA_{94}$ worms at various sunflower oil volume fractions.

Next we investigated whether the shear rate affected the mean droplet diameter. Six emulsions were prepared at 20 ºC using equal volumes of sunflower oil and methanol via homogenization

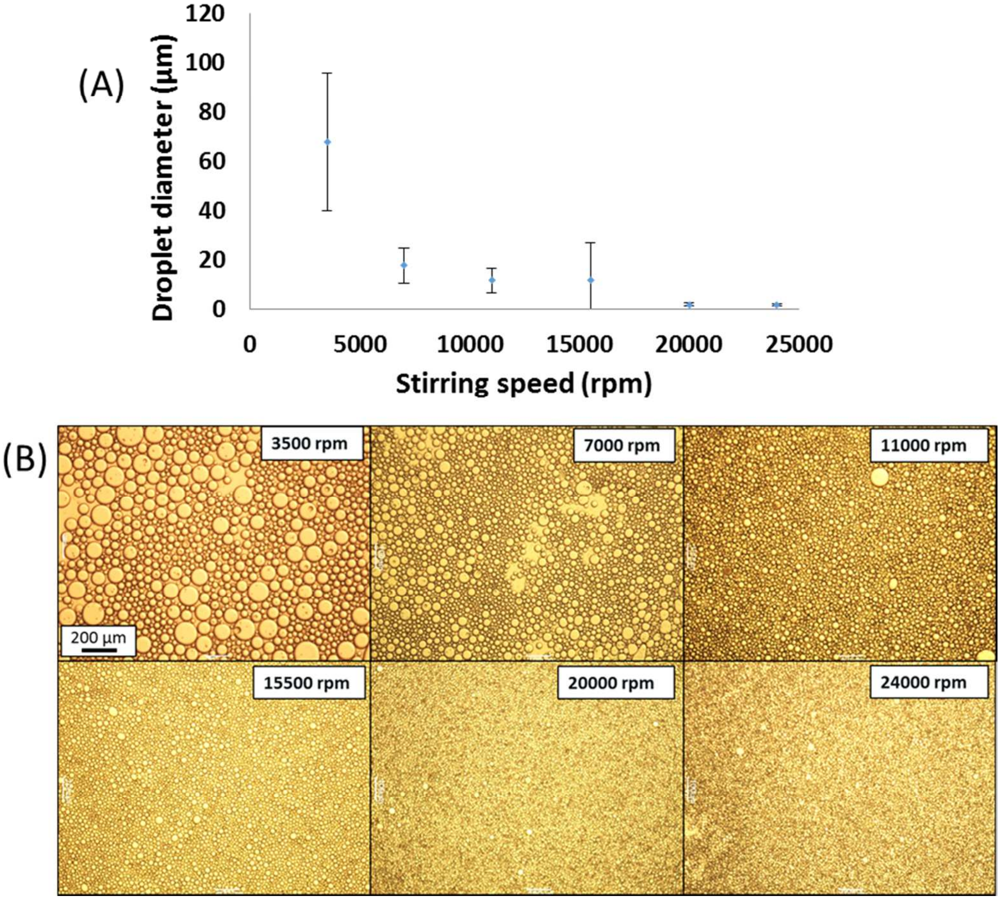

Fig. 4 (A) Mean laser diffraction droplet diameter versus stirring speed for sunflower oil-in-methanol emulsions prepared with 0.66 % w/w $PDMA_{43}$-$PBzMA_{94}$ worms using equal volumes of methanol and sunflower oil. The error bars represent the standard deviation of each mean volume-average droplet diameter, rather than the experimental error. (B) Optical microscopy images recorded for homogenization at stirring speeds of between 3500 rpm and 24000 rpm. The 200 µm scale bar in the first image applies to all images

Table 2 Effect of varying the PDMA$_{43}$-PBzMA$_{94}$ worm concentration on the mean droplet diameter, fractional surface coverage (C_w) and the adsorption efficiency of the worms on the sunflower oil droplets

Concentration	Initial emulsion after 24 h			Aged emulsion after 7 days			Aged emulsions after 2 months
	Mean laser diffraction droplet diameter (µm)	C_w	Pickering emulsion adsorption efficiency (%)	Mean laser diffraction droplet diameter (µm)	C_w	Pickering emulsion adsorption efficiency (%)	Mean laser diffraction droplet diameter (µm)
1.32% w/w	9 ± 5	0.85	99	37 ± 30	2.12	60	40 ± 32
0.66% w/w	9 ± 6	0.42	98	39 ± 21	1.25	67	39 ± 16
0.33% w/w	14 ± 7	0.33	97	43 ± 18	0.82	80	44 ± 17
0.04% w/w	48 ± 28	0.13	91	77 ± 31	0.19	85	79 ± 29
0.02% w/w	53 ± 28	0.06	82	116 ± 60	0.11	68	104 ± 67

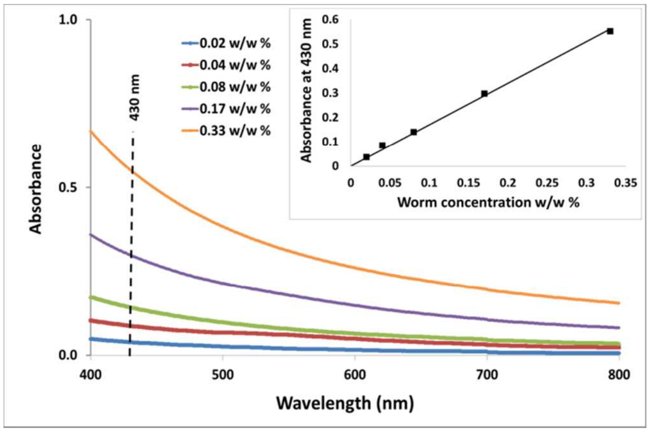

Fig. 5 Visible absorption spectra recorded for methanolic dispersions of PDMA$_{43}$-PBzMA$_{94}$ worms at various concentrations between 400 and 800 nm. An arbitrary wavelength of 430 nm was used to construct a linear calibration plot (see inset), which was used to determine the concentration of free copolymer worms present in the methanol continuous phase, after emulsification and subsequent sedimentation of the relatively dense sunflower oil droplets

for two minutes using stirring speeds ranging between 3500 rpm and 24000 rpm. Figure 4 shows that the droplet diameter is significantly reduced at higher stirring speeds. This was expected, as greater shear creates a higher droplet surface area.

The fractional surface coverage, C_w, for the worms adsorbed onto the sunflower oil droplets was calculated by dividing the total surface area of the adsorbed worms by the total surface area of the droplets to afford Equation (1), as reported previously by Kalashnikova and co-workers[82].

$$C_w = \frac{m_p D}{6 \rho_p h_p V_d} \qquad (1)$$

The mean droplet diameter, D, was determined by laser diffraction, m_p is the nanoparticle mass, ρ_p is the nanoparticle density (1.15 g cm^{-3} for the PBzMA core-forming block, as determined by helium pycnometry) and V_d is the total volume of the oil droplet phase (which is 5.0 ml in these experiments). In this case h_p represents the mean worm thickness of 20 nm, as estimated from TEM images. The fractional surface coverages, C_w, calculated for the various worm-stabilized emulsions are summarized in Table 2. These C_w values are typically less than unity, but in two cases they exceed unity. This is interpreted as evidence for (partial) bilayer formation, as previously reported by Kalashnikova et al. for similarly anisotropic cellulosic nanocrystals [40,82]. In each case the adsorption efficiency of the particles was determined 24 h after initial emulsification using turbidimetry at an arbitrary fixed wavelength of 430 nm, see Figure 5. This time period was sufficient to ensure complete sedimentation of the relatively dense sunflower oil droplets, leaving only non-adsorbed worms in the methanolic continuous phase. The adsorption efficiency indicates the proportion of the initial worms that actually become adsorbed at the droplet surface. This efficiency is reduced from 99 % to 82 % on lowering the worm concentration. The mean droplet diameter increased significantly for up to four days after homogenization, before attaining a constant value. Turbidimetry studies were repeated seven days after homogenization (i.e. long after the droplet diameter had stabilized) these data showed the worm adsorption efficiency had *decreased*. However, no significant change in worm adsorption efficiency was observed thereafter, while laser diffraction studies of emulsions aged for several months at 20 ˚C confirmed their long-term droplet stability.

We postulate the following mechanism to account for our experimental observations. After initial homogenization, the surface of the droplets is only partially covered by the worms, which have a relatively high adsorption efficiency. Thus the droplets are able to undergo limited coalescence, which lowers the total interfacial area and hence increases the fractional surface coverage, C_w, of the sunflower oil droplets, see Figure 6. Coalescence no longer occurs when the droplet surface is sufficiently coated by the worms. Indeed, the fractional surface coverages calculated for the seven-day aged emulsions are significantly greater than the corresponding initial C_w values, see Table 2. This suggests that the worm fractional surface coverage gradually increases as the emulsion ages. There is a concomitant reduction in the worm adsorption efficiency, indicating *desorption* of some of the worms from the droplet surface into the continuous phase, see Figure 6.

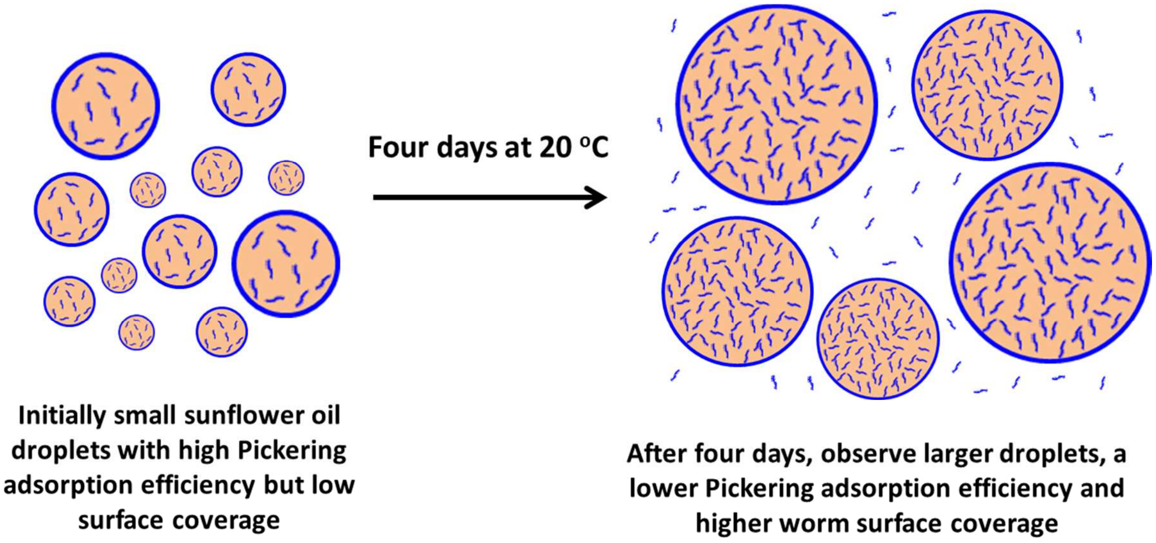

Fig. 6 Proposed mechanism for the observed increase in mean droplet diameter for PDMA$_{43}$-PBzMA$_{94}$ worm-stabilized sunflower oil-in-methanol Pickering emulsions. The initial droplets formed immediately after emulsification are relatively small, with a patchy coating of worms adsorbed at the methanol-sunflower oil interface with relatively high efficiencies (82-99%). On ageing for approximately four days, some of the initial droplets undergo limited coalescence to form appreciably larger droplets, with a rather higher fractional surface coverage of adsorbed worms and a significant fraction of non-adsorbed worms now residing in the methanolic continuous phase. This coarser emulsion remained stable for at least several months.

In principle, an alternative mechanism for the observed increase in emulsion size could be Ostwald ripening. According to Weidner and co-workers, the solubility of sunflower oil in methanol is approximately 0.5-1.0 % w/w at 20˚C [83]. Thus Ostwald ripening might occur for the present Pickering emulsion formulation via gradual diffusion of the sparingly soluble sunflower oil from smaller to larger droplets. However, this explanation does not appear to be consistent with the experimental observations. Interfacial adsorption of the worms is expected to be strong and essentially irreversible. Thus, if such sunflower oil diffusion occurred, both an increase in mean droplet diameter and a *reduction* in C_w would be expected. In practice, only the former change is observed – the worm surface coverage actually *increases* as the emulsion coarsens on ageing. In summary, we suggest that the increase in emulsion droplet dimensions over time is most likely the result of a limited coalescence mechanism. However, one reviewer of this manuscript has suggested that our experimental observations may be consistent with Ostwald ripening, provided that the worms released after preferential dissolution of the smaller droplets are partially readsorbed onto the growing larger droplets. It seems that further studies are warranted to clarify the true situation, but unfortunately this is beyond the scope of the present study.

The spontaneous formation of methanol-in-sunflower oil-in-methanol Pickering double emulsions was also observed, see Figure 7. The presence of such double emulsions was confirmed by optical microscopy studies of freshly prepared emulsions at all worm concentrations used in this work (0.02 % w/w to 2.65 % w/w). However, when the aged emulsions were re-examined after seven days (i.e. after limited coalescence had occurred), double emulsions were *only* observed for emulsions prepared at the higher worm concentrations (0.66, 1.35 and 2.65 % w/w). In these three cases, a significant proportion of double emulsion droplets were still present, indicating that such double emulsions are stable beyond the period of droplet coalescence, see Figure 7. The precise mechanism of this double emulsion formation is not understood at the present time, but clearly warrants further studies.

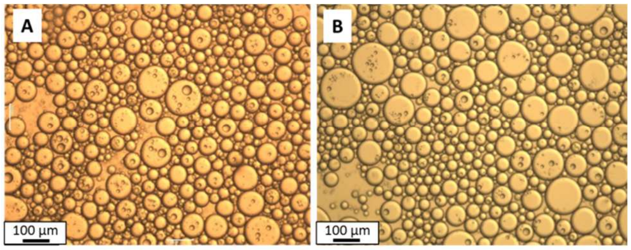

Fig. 7 Optical microscopy images indicating the presence of methanol-in-sunflower oil-in-methanol double emulsions within a sunflower oil-in-methanol emulsion prepared by homogenizing a methanolic dispersion of 0.66 % w/w PDMA$_{43}$-PBzMA$_{94}$ worms with an equal volume of sunflower oil for 2 minutes at a stirring speed of 13500 rpm at 20 ˚C. (A) immediately after homogenization and (B) after ageing for seven days

Conclusions

Sunflower oil-in-methanol Pickering emulsions can be prepared using PDMA$_{43}$-PBzMA$_{94}$ diblock copolymer worms as Pickering emulsifiers. Increasing the particle concentration allows stabilization of smaller droplets (< 10 µm at 1.32 % w/w) however emulsions formed at particle concentrations as low as 0.02 % w/w were still stable (average droplet diameter 53 µm). Systematically varying the stirring speed during homogenization produced emulsions with adjustable diameters up to a sunflower oil volume fraction of 0.60. Turbidimetry studies were employed to assess Pickering adsorption efficiency and an appreciable increase in mean droplet diameter was observed on ageing at ambient temperature. On closer inspection, no further increase in droplet diameter occurred after around four days. At all worm concentrations investigated, Pickering adsorption efficiencies were lower for seven-day-old emulsions than for the initial emulsion, while the worm fractional surface coverage increased significantly on this time scale. After this ageing period, the droplet diameter remains essentially unchanged for at least two months. Based on these experimental observations, we suggest that this increase in droplet diameter is the result of limited coalescence. Methanol-in-sunflower oil-in-methanol double emulsion droplets were also observed for this non-aqueous Pickering emulsion formulation and this observation warrants further studies.

Acknowledgments. We thank DSM Advanced Surfaces (Geleen, The Netherlands) and EPSRC for a CASE PHD studentship for ERJ. SPA thanks EPSRC (Platform grant EP/J007846/1) for partial post-doctoral support of KLT and also acknowledges a five-year Advanced Investigator ERC grant (PISA 320372) and partial project funding from Stichting Innovatie Alliantie (Foundation Innovation Alliance).

References

1. Ramsden W (1903) "Separation of solids in the surface-layers of solutions and 'Suspensions' (Observations on surface-membranes, bubbles, emulsions, and mechanical coagulation). Preliminary Account.". Proc R Soc London 72 (479):156-164. doi:10.1098/rspl.1903.0034

2. Pickering SU (1907) Emulsions. J Chem Soc 91:2001-2021. doi:10.1039/ct9079102001

3. Levine S, Bowen BD, Partridge SJ (1989) Stabilization of emulsions by fine particles .1. Partitioning effect of particles between continuous phase and oil-water interface. Colloids and Surfaces 38 (4):325-343. doi:10.1016/0166-6622(89)80271-9

4. Binks BP, Lumsdon SO (1999) Stability of oil-in-water emulsions stabilised by silica particles. PCCP 1 (12):3007-3016. doi:10.1039/a902209k

5. Binks BP, Lumsdon SO (2000) Effects of oil type and aqueous phase composition on oil-water mixtures containing particles of intermediate hydrophobicity. PCCP 2 (13):2959-2967. doi:10.1039/b002582h

6. Binks BP, Whitby CP (2004) Silica particle-stabilized emulsions of silicone oil and water: Aspects of emulsification. Langmuir 20 (4):1130-1137. doi:10.1021/la0303557

7. Gautier F, Destribats M, Perrier-Cornet R, Dechezelles JF, Giermanska J, Heroguez V, Ravaine S, Leal-Calderon F, Schmitt V (2007) Pickering emulsions with stimulable particles: from highly- to weakly-covered interfaces. PCCP 9 (48):6455-6462. doi:10.1039/b710226g

8. Lagaly G, Reese M, Abend S (1999) Smectites as colloidal stabilizers of emulsions - I. Preparation and properties of emulsions with smectites and nonionic surfactants. Appl Clay Sci 14 (1-3):83-103. doi:10.1016/s0169-1317(98)00051-9

9. Binks BP, Clint JH, Whitby CP (2005) Rheological behavior of water-in-oil emulsions stabilized by hydrophobic bentonite particles. Langmuir 21 (12):5307-5316. doi:10.1021/la050255w

10. Bon SAF, Colver PJ (2007) Pickering miniemulsion polymerization using Laponite clay as a stabilizer. Langmuir 23 (16):8316-8322. doi:10.1021/la701150q

11. Guillot S, Bergaya F, de Azevedo C, Warmont F, Tranchant JF (2009) Internally structured pickering emulsions stabilized by clay mineral particles. J Colloid Interface Sci 333 (2):563-569. doi:10.1016/j.jcis.2009.01.026

12. Cui YN, Threlfall M, van Duijneveldt JS (2011) Optimizing organoclay stabilized Pickering emulsions. J Colloid Interface Sci 356 (2):665-671. doi:10.1016/j.jcis.2011.01.046

13. Velev OD, Furusawa K, Nagayama K (1996) Assembly of latex particles by using emulsion droplets as templates .1. Microstructured hollow spheres. Langmuir 12 (10):2374-2384. doi:10.1021/la9506786

14. Binks BP, Lumsdon SO (2001) Pickering emulsions stabilized by monodisperse latex particles: Effects of particle size. Langmuir 17 (15):4540-4547. doi:10.1021/la0103822

15. Laib S, Routh AF (2008) Fabrication of colloidosomes at low temperature for the encapsulation of thermally sensitive compounds. J Colloid Interface Sci 317 (1):121-129. doi:10.1016/j.jcis.2007.09.019

16. Walsh A, Thompson KL, Armes SP, York DW (2010) Polyamine-Functional Sterically Stabilized Latexes for Covalently Cross-Linkable Colloidosomes. Langmuir 26 (23):18039-18048. doi:10.1021/la103804y

17. Thompson KL, Armes SP (2010) From well-defined macromonomers to sterically-stabilised latexes to covalently cross-linkable colloidosomes: exerting control over multiple length scales. Chem Commun 46 (29):5274-5276. doi:10.1039/c0cc01362e

18. Atanase LI, Riess G (2013) Block copolymer stabilized nonaqueous biocompatible sub-micron emulsions for topical applications. Int J Pharm 448 (2):339-345. doi:10.1016/j.ijpharm.2013.03.051

19. Binks BP, Lumsdon SO (2000) Influence of particle wettability on the type and stability of surfactant-free emulsions. Langmuir 16 (23):8622-8631. doi:10.1021/la000189s

20. Binks BP (2002) Particles as surfactants - similarities and differences. Current Opinion in Colloid & Interface Science 7 (1-2):21-41. doi:10.1016/s1359-0294(02)00008-0

21. Aveyard R, Binks BP, Clint JH (2003) Emulsions stabilised solely by colloidal particles. Adv Colloid Interface Sci 100:503-546. doi:10.1016/s0001-8686(02)00069-6

22. McMahon JD, Hamill RD, Petersen RV (1963) Emulsifying effects of several ionic surfactants on a nonaqueous immiscible system. J Pharm Sci 52 (12):1163-&. doi:10.1002/jps.2600521214

23. Molau GE (1965) Heterogeneous polymer systems .I. Polymeric oil-in-oil emulsions. Journal of Polymer Science Part a-General Papers 3 (4PA):1267-&. doi:10.1002/pol.1965.100030402

24. Periard J, Banderet A, Riess G (1970) Emulsifying effect of block and graft copolymers - Oil-in-oil emulsions. Journal of Polymer Science Part B-Polymer Letters 8 (2):109-&. doi:10.1002/pol.1970.110080210

25. Crespy D, Landfester K (2011) Making dry fertile: a practical tour of non-aqueous emulsions and miniemulsions, their preparation and some applications. Soft Matter 7 (23):11054-11064. doi:10.1039/c1sm06156a

26. Klapper M, Nenov S, Haschick R, Müller K, Müllen K (2008) Oil-in-Oil Emulsions: A Unique Tool for the Formation of Polymer Nanoparticles. Acc Chem Res 41 (9):1190-1201. doi:10.1021/ar8001206

27. Jackson WM, Drury JS (1959) Miscibility of organic solvent pairs. Ind Eng Chem 51 (12):1491-1493. doi:10.1021/ie50600a039

28. Imhof A, Pine DJ (1997) Ordered macroporous materials by emulsion templating. Nature 389 (6654):948-951. doi:10.1038/40105

29. Crespy D, Landfester K, Schubert US, Schiller A (2010) Potential photoactivated metallopharmaceuticals: from active molecules to supported drugs. Chem Commun 46 (36):6651-6662. doi:10.1039/c0cc01887b

30. Crespy D, Landfester K (2009) Synthesis of polyvinylpyrrolidone/silver nanoparticles hybrid latex in non-aqueous miniemulsion at high temperature. Polymer 50 (7):1616-1620. doi:10.1016/j.polymer.2009.02.003

31. Jaitely V, Sakthivel T, Magee G, Florence AT (2004) Formulation of oil in oil emulsions: potential drug reservoirs for slow release. J Drug Deliv Sci Technol 14 (2):113-117. doi:10.1016/S1773-2247(04)50022-9

32. Dorresteijn R, Ragg R, Rago G, Billecke N, Bonn M, Parekh SH, Battagliarin G, Peneva K, Wagner M, Klapper M, Mullen K (2013) Biocompatible Polylactide-block-Polypeptide-block-Polylactide Nanocarrier. Biomacromolecules 14 (5):1572-1577. doi:10.1021/bm400216r

33. Noble PF, Cayre OJ, Alargova RG, Velev OD, Paunov VN (2004) Fabrication of "hairy" colloidosomes with shells of polymeric microrods. J Am Chem Soc 126 (26):8092-8093. doi:10.1021/ja047808u

34. Alargova RG, Warhadpande DS, Paunov VN, Velev OD (2004) Foam superstabilization by polymer microrods. Langmuir 20 (24):10371-10374. doi:10.1021/la048647a

35. Thompson KL, Mable CJ, Cockram A, Warren NJ, Cunningham VJ, Jones ER, Verber R, Armes SP (2014) Are block copolymer worms more effective Pickering emulsifiers than block copolymer spheres? Soft Matter 10 (43):8615-8626. doi:10.1039/c4sm01724b

36. Thompson KL, Fielding LA, Mykhaylyk OO, Lane JA, Derry MJ, Armes SP (2015) Vermicious Thermo-responsive Pickering Emulsifiers. Chemical Science. doi:10.1039/C5SC00598A

37. Andresen M, Stenius P (2007) Water-in-oil emulsions stabilized by hydrophobized microfibrillated cellulose. J Dispersion Sci Technol 28 (6):837-844. doi:10.1080/01932690701341827

38. Madivala B, Fransaer J, Vermant J (2009) Self-Assembly and Rheology of Ellipsoidal Particles at Interfaces. Langmuir 25 (5):2718-2728. doi:10.1021/la803554u

39. Madivala B, Vandebril S, Fransaer J, Vermant J (2009) Exploiting particle shape in solid stabilized emulsions. Soft Matter 5 (8):1717-1727. doi:10.1039/b816680c

40. Kalashnikova I, Bizot H, Bertoncini P, Cathala B, Capron I (2013) Cellulosic nanorods of various aspect ratios for oil in water Pickering emulsions. Soft Matter 9 (3):952-959. doi:10.1039/c2sm26472b

41. Hawker CJ (1994) Molecular-weight control by a living free-radical polymerization process. J Am Chem Soc 116 (24):11185-11186. doi:10.1021/ja00103a055

42. Wang JS, Matyjaszewski K (1995) Controlled living radical polymerization - halogen atom-transfer radical polymerization promoted by a CU(I)CU(II) redox process. Macromolecules 28 (23):7901-7910. doi:10.1021/ma00127a042

43. Chiefari J, Chong YK, Ercole F, Krstina J, Jeffery J, Le TPT, Mayadunne RTA, Meijs GF, Moad CL, Moad G, Rizzardo E, Thang SH (1998) Living Free-Radical Polymerization by Reversible Additionâˆ’Fragmentation Chain Transfer: The RAFT Process. Macromolecules 31 (16):5559-5562. doi:10.1021/ma9804951

44. Benoit D, Chaplinski V, Braslau R, Hawker CJ (1999) Development of a universal alkoxyamine for "living" free radical polymerizations. J Am Chem Soc 121 (16):3904-3920. doi:10.1021/ja984013c

45. Kamigaito M, Ando T, Sawamoto M (2001) Metal-catalyzed living radical polymerization. Chem Rev 101 (12):3689-3745. doi:10.1021/cr9901182

46. Braunecker WA, Matyjaszewski K (2007) Controlled/living radical polymerization: Features, developments, and perspectives. Prog Polym Sci 32 (1):93-146. doi:10.1016/j.progpolymsci.2006.11.002

47. Qiu J, Charleux B, Matyjaszewski K (2001) Controlled/living radical polymerization in aqueous media: homogeneous and heterogeneous systems. Prog Polym Sci 26 (10):2083-2134. doi:10.1016/s0079-6700(01)00033-8

48. An ZS, Shi QH, Tang W, Tsung CK, Hawker CJ, Stucky GD (2007) Facile RAFT precipitation polymerization for the microwave-assisted synthesis of well-defined, double hydrophilic block copolymers and nanostructured hydrogels. J Am Chem Soc 129 (46):14493-14499. doi:10.1021/ja0756974

49. Cunningham MF (2008) Controlled/living radical polymerization in aqueous dispersed systems. Prog Polym Sci 33 (4):365-398. doi:http://dx.doi.org/10.1016/j.progpolymsci.2007.11.002

50. Rieger J, Stoffelbach F, Bui C, Alaimo D, Jerome C, Charleux B (2008) Amphiphilic poly(ethylene oxide) macromolecular RAFT agent as a stabilizer and control agent in ab initio batch emulsion polymerization. Macromolecules 41 (12):4065-4068. doi:10.1021/ma800544v

51. Petzetakis N, Dove AP, O'Reilly RK (2011) Cylindrical micelles from the living crystallization-driven self-assembly of poly(lactide)-containing block copolymers. Chemical Science 2 (5):955-960. doi:10.1039/c0sc00596g

52. Sugihara S, Blanazs A, Armes SP, Ryan AJ, Lewis AL (2011) Aqueous Dispersion Polymerization: A New Paradigm for in Situ Block Copolymer Self-Assembly in Concentrated Solution. J Am Chem Soc 133 (93):15707-15713. doi:10.1021/ja205887v

53. Delaittre G, Save M, Gaborieau M, Castignolles P, Rieger J, Charleux B (2012) Synthesis by nitroxide-mediated aqueous dispersion polymerization, characterization, and physical core-crosslinking of pH- and thermoresponsive dynamic diblock copolymer micelles. Polymer Chemistry 3 (6):1526-1538. doi:10.1039/c2py20084h

54. Warren NJ, Armes SP (2014) Polymerization-Induced Self-Assembly of Block Copolymer Nano-objects via RAFT Aqueous Dispersion Polymerization. J Am Chem Soc 136 (29):10174-10185. doi:10.1021/ja502843f

55. Cai W, Wan W, Hong C, Huang C, Pan C-Y (2010) Morphology transitions in RAFT polymerization. Soft Matter 6 (21):5554-5561. doi:10.1039/C0SM00284D

56. Blanazs A, Madsen J, Battaglia G, Ryan AJ, Armes SP (2011) Mechanistic Insights for Block Copolymer Morphologies: How Do Worms Form Vesicles? J Am Chem Soc 133 (41):16581-16587. doi:10.1021/ja206301a

57. Charleux B, Delaittre G, Rieger J, D'Agosto F (2012) Polymerization-Induced Self-Assembly: From Soluble Macromolecules to Block Copolymer Nano-Objects in One Step. Macromolecules 45 (17):6753-6765. doi:10.1021/ma300713f

58. Semsarilar M, Jones ER, Blanazs A, Armes SP (2012) Efficient Synthesis of Sterically-Stabilized Nano-Objects via RAFT Dispersion Polymerization of Benzyl Methacrylate in Alcoholic Media. Adv Mater 24 (25):3378-3382. doi:10.1002/adma.201200925

59. Fielding LA, Derry MJ, Ladmiral V, Rosselgong J, Rodrigues AM, Ratcliffe LPD, Sugihara S, Armes SP (2013) RAFT dispersion polymerization in non-polar solvents: facile production of block copolymer spheres, worms and vesicles in n-alkanes. Chemical Science 4:2081-2087. doi:10.1039/C3SC50305D

60. Blanazs A, Armes SP, Ryan AJ (2009) Self-Assembled Block Copolymer Aggregates: From Micelles to Vesicles and their Biological Applications. Macromol Rapid Commun 30 (4-5):267-277. doi:10.1002/marc.200800713

61. Monteiro MJ, Cunningham MF (2012) Polymer Nanoparticles via Living Radical Polymerization in Aqueous Dispersions: Design and Applications. Macromolecules 45 (12):4939-4957. doi:10.1021/ma300170c

62. Wan W-M, Pan C-Y (2010) One-pot synthesis of polymeric nanomaterials via RAFT dispersion polymerization induced self-assembly and re-organization. Polymer Chemistry 1 (9):1475-1484. doi:10.1039/C0PY00124D

63. Huang C-Q, Pan C-Y (2010) Direct preparation of vesicles from one-pot RAFT dispersion polymerization. Polymer 51 (22):5115-5121. doi:10.1016/j.polymer.2010.08.056

64. Jones ER, Semsarilar M, Blanazs A, Armes SP (2012) Efficient Synthesis of Amine-Functional Diblock Copolymer Nanoparticles via RAFT Dispersion Polymerization of Benzyl Methacrylate in Alcoholic Media. Macromolecules 45 (12):5091-5098. doi:10.1021/ma300898e

65. Gonzato C, Semsarilar M, Jones ER, Li F, Krooshof GJP, Wyman P, Mykhaylyk OO, Tuinier R, Armes SP (2014) Rational Synthesis of Low-Polydispersity Block Copolymer Vesicles in Concentrated Solution via Polymerization-Induced Self-Assembly. J Am Chem Soc 136 (31):11100-11106. doi:10.1021/ja505406s

66. Houillot L, Bui C, Save M, Charleux B, Farcet C, Moire C, Raust JA, Rodriguez I (2007) Synthesis of well-defined polyacrylate particle dispersions in organic medium using simultaneous RAFT polymerization and self-assembly of block copolymers. A strong influence of the selected thiocarbonylthio chain transfer agent. Macromolecules 40 (18):6500-6509. doi:10.1021/ma0703249

67. Fielding LA, Lane JA, Derry MJ, Mykhaylyk OO, Armes SP (2014) Thermo-responsive Diblock Copolymer Worm Gels in Non-polar Solvents. J Am Chem Soc 136 (15):5790-5798. doi:10.1021/ja501756h

68. Bernard J, Save M, Arathoon B, Charleux B (2008) Preparation of a xanthate-terminated dextran by click chemistry: Application to the synthesis of polysaccharide-coated nanoparticles via surfactant-free <I>ab initio</I> emulsion polymerization of vinyl acetate. J Polym Sci, Part A: Polym Chem 46 (8):2845-2857. doi:10.1002/pola.22618

69. Rieger J, Osterwinter G, Bui CO, Stoffelbach F, Charleux B (2009) Surfactant-Free Controlled/Living Radical Emulsion (Co)polymerization of n-Butyl Acrylate and Methyl Methacrylate via RAFT Using

Amphiphilic Poly(ethylene oxide)-Based Trithiocarbonate Chain Transfer Agents. Macromolecules 42 (15):5518-5525. doi:10.1021/ma9008803

70. Rieger J, Zhang W, Stoffelbach Fo, Charleux B (2010) Surfactant-Free RAFT Emulsion Polymerization Using Poly(N,N-dimethylacrylamide) Trithiocarbonate Macromolecular Chain Transfer Agents. Macromolecules 43 (15):6302-6310. doi:10.1021/ma1009269

71. Boissé S, Rieger J, Pembouong G, Beaunier P, Charleux B (2011) Influence of the stirring speed and CaCl2 concentration on the nano-object morphologies obtained via RAFT-mediated aqueous emulsion polymerization in the presence of a water-soluble macroRAFT agent. J Polym Sci, Part A: Polym Chem 49 (15):3346-3354. doi:10.1002/pola.24771

72. Zhang W, D'Agosto F, Boyron O, Rieger J, Charleux B (2011) One-Pot Synthesis of Poly(methacrylic acid-co-poly(ethylene oxide) methyl ether methacrylate)-b-polystyrene Amphiphilic Block Copolymers and Their Self-Assemblies in Water via RAFT-Mediated Radical Emulsion Polymerization. A Kinetic Study. Macromolecules 44 (19):7584-7593. doi:10.1021/ma201515n

73. Zhang X, Boissé S, Zhang W, Beaunier P, D'Agosto F, Rieger J, Charleux B (2011) Well-Defined Amphiphilic Block Copolymers and Nano-objects Formed in Situ via RAFT-Mediated Aqueous Emulsion Polymerization. Macromolecules 44 (11):4149-4158. doi:10.1021/ma2005926

74. Zhang W, D'Agosto F, Boyron O, Rieger J, Charleux B (2012) Toward a Better Understanding of the Parameters that Lead to the Formation of Nonspherical Polystyrene Particles via RAFT-Mediated One-Pot Aqueous Emulsion Polymerization. Macromolecules 45 (10):4075-4084. doi:10.1021/ma300596f

75. Sun JT, Hong CY, Pan CY (2013) Recent advances in RAFT dispersion polymerization for preparation of block copolymer aggregates. Polymer Chemistry 4 (4):873-881. doi:10.1039/c2py20612a

76. Zong MM, Thurecht KJ, Howdle SM (2008) Dispersion polymerisation in supercritical CO(2) using macro-RAFT agents. Chem Commun (45):5942-5944. doi:10.1039/b812827h

77. Boissé S, Rieger J, Belal K, Di-Cicco A, Beaunier P, Li M-H, Charleux B (2010) Amphiphilic block copolymer nano-fibers via RAFT-mediated polymerization in aqueous dispersed system. Chem Commun 46 (11):1950-1952. doi:10.1039/B923667H

78. Zhang X, Boissé S, Bui C, Albouy P-A, Brulet A, Li M-H, Rieger J, Charleux B (2012) Amphiphilic liquid-crystal block copolymer nanofibers via RAFT-mediated dispersion polymerization. Soft Matter 8 (4):1130-1141. doi:10.1039/C1SM06598J

79. Semsarilar M, Ladmiral V, Blanazs A, Armes SP (2012) Anionic Polyelectrolyte-Stabilized Nanoparticles via RAFT Aqueous Dispersion Polymerization. Langmuir 28 (1):914-922. doi:10.1021/la203991y

80. Zhang X, Rieger J, Charleux B (2012) Effect of the solvent composition on the morphology of nano-objects synthesized via RAFT polymerization of benzyl methacrylate in dispersed systems. Polymer Chemistry 3:1502-1509. doi:10.1039/C2PY20071F

81. Thompson KL, Lane JA, Derry MJ, Armes SP (2015) Non-aqueous Isorefractive Pickering Emulsions. Langmuir 31 (15):4373-4376. doi:10.1021/acs.langmuir.5b00630

82. Kalashnikova I, Bizot H, Cathala B, Capron I (2011) New Pickering Emulsions Stabilized by Bacterial Cellulose Nanocrystals. Langmuir 27 (12):7471-7479. doi:10.1021/la200971f

83. Cerce T, Peter S, Weidner E (2005) Biodiesel-transesterification of biological oils with liquid catalysts: Thermodynamic properties of oil-methanol-amine mixtures. Industrial & Engineering Chemistry Research 44 (25):9535-9541. doi:10.1021/ie050252e

Preparation of Non-Aqueous Pickering Emulsions Using Anisotropic Block Copolymer Nanoparticles

S. L. Rizzelli, E. R. Jones, K. L. Thompson and S. P. Armes*

*Department of Chemistry, Dainton Building, University of Sheffield, Brook Hill, Sheffield, Yorkshire, S3 7HF, UK., e-mail: s.p.armes@sheffield.ac.uk

Figure S1. Optical microscopy images recorded for sunflower oil-in-methanol Pickering emulsions prepared using PDMA$_{43}$-PBzMA$_{94}$ worms at concentrations between 2.65 and 0.01 % w/w ((A) 2.65% w/w, (B) 1.32 % w/w, (C) 0.66 % w/w, (D) 0.17 % w/w, (E) 0.08 % w/w and (F) 0.01 % w/w). Emulsions were prepared by homogenising particles with an equal volume of sunflower oil at 13500 rpm at 20˚C for 2 minutes. The 100 µm scale bar in the first image applies to all images.